CoA. Note Mat. No. 3

THE COLLEGE OF AERONAUTICS

CRANFIELD

ANISOTROPIC CREEP IN A GLASS-FIBRE LAMINATE

by

A. Kaye and D.W. Saunders

CoA Note Mat. No. 3

April, 1964

THE COLLEGE OF AERONAUTICS

DEPARTMENT OF MATERIALS

Anisotropic creep in a glass-fibre laminate

- by -

A. Kaye, M.A., A.Inst.P.

and

D.W. Saunders, Ph.D., B.Sc., A.R.C.S., F.Inst.P.

SUMMARY

A glass fibre epoxy resin laminate was prepared from a flexible thermosetting resin and a 'plain weave' glass cloth. Experiments in simple tensile creep were carried out on strips cut with their long dimensions at various angles to the warp threads in the glass cloth. It was found that each of these strips showed, over the limited range of loads and times covered, essentially linear creep behaviour. The creep compliance varied systematically with direction being as much as twenty times smaller in the warp and weft directions as at 45° to these directions. It was found that the shape of the creep compliance versus orientation curves was similar for all times and the behaviour can therefore conveniently be described by two curves, a master curve of reduced creep compliance as a function of direction and a curve of reduction factor versus time.

The significance of both these curves is discussed in terms of an extension of linear viscoelasticity theory to the case of antisotropic materials. It is shown that the variation of creep compliance with direction is similar in form to the variation of elastic compliance with direction in orthorhombic anisotropic elastic materials and also that the results are consistent with a similar variation of relaxation time spectrum with direction.

Contents

Introduction

The linear theories of viscoelasticity as presented by Gross (1953), Ferry (1961) and other workers are commonly restricted to the incompressible isotropic case. Extensions to take into account bulk (volume) effects have been proposed and some experimental work has been reported to investigate such effects in real materials.

Interest in viscoelastic behaviour in anisotropic media is however, not well developed. Biot (1954) has investigated the matter theoretically.

In this paper some results of creep measurements on a fibre-glass-resin laminate, which might be expected to approximate to orthorhombic symmetry in its mechanical properties, are presented. The results are discussed in terms of some simple extensions of isotropic linear viscoelastic theory.

Materials

The glass fibre laminate was prepared from a plain weave glass cloth (Marglass 121T finish P.703) of density 2.54 gm/cc with 27 threads/inch in both warp and weft. The resin employed was a flexible epoxy resin made up of 60 parts by weight of Bakelite resin R18774 with 40 parts of flexibiliser DQ19116.

The laminates were prepared in 9 inch by 9 inch squares each containing 13 layers of glass cloth. The cloth squares were carefully laid with their warps parallel and stapled together. The individual pieces of cloths were then fully impregnated with the resin by hand and the whole cured at about 80°C for 24 hours in a hot press in a suitable mould. The density of the laminate was 1.70 gms/cc compared with a resin density of 1.13 gms/cc and a glass density of 2.54 gms/cc.

The laminate thickness was approximately $^1/_8$ inch.

Experimental

Strips approximately $\frac{1}{2}$ inch wide and 6 inches long were cut from the laminates with their long dimensions making angles of 0, 15, 30, 45, 60, 75 and 90 degrees to the warp direction of the glass cloth.

Each strip of laminate was subjected to a series of creep and recovery experiments at various constant loads.

The strip was clamped at its upper end to a rigid support. A further clamp at the lower end of the sample supported a small lightweight carrier to which deadweight creep loads could be added.

Extensions in the sample were observed using a Lamb extensometer having a gauge length of 2 inches and a sensitivity such that a strain of 10^{-3} could be measured to 1%.

The whole apparatus was enclosed in an air thermostat which gave temperature control to ± 1°C.

The following procedure was adopted. The smallest creep load was applied at the time taken as zero time and creep observed for a period of 2 minutes. The specimen was then allowed to relax, free of load, for a further period of 1 hour after which the next highest creep load was applied and the cycle repeated. Seven cycles, with increasing loads, were carried out on each sample.

The dimensions of each sample were measured with a travelling microscope and micrometer gauge.

Results

The temperature dependence of the creep curves was greater than had been expected and the degree of temperature control achieved (viz. ± 1°C) was barely adequate. In view of this, care was taken to begin each creep curve at the same temperature but undoubtedly variations of temperature did result in some scatter in the results.

A further source of error derived from the use of the Lamb extensometer. It was found that the forces needed to operate the extensometer were not negligibly small compared with the creep loads; this results in the stress-strain curves for a given time not passing through the origin. A first correction for this error has been applied by subtracting the load at zero deformation (obtained by extrapolation of the stress-strain relations to zero strain) from the applied load to give the effective creep load. The results are presented in terms of this effective creep load.

In Figure 1 the creep data obtained on a sample cut from the sheet with its long direction at 30° to the warp direction are presented. The figure shows creep strain at various given times after application of the creep load plotted against the (effective) creep load. These curves were obtained by interpolation from ordinary creep curves. The results are typical of the behaviour of other samples in that they show that at loads less than 1 kg the load deformation relations are essentially linear.

It follows that for sufficiently low loads the creep behaviour of the samples may be represented by a creep compliance $J(t,\theta)$ defined as the creep strain per unit (effective) applied creep stress. t is the time of creep in seconds and θ the angle of orientation of the long dimension of the sample relative to the warp threads. (Since the creep strains are small we shall ignore the distinction between creep at constant load and creep at constant stress; in fact the creep compliances are all computed with reference to the initial creep stress, i.e. the unstrained cross sectional area).

The creep compliances were obtained simply from the slopes of the load-deformation curves in the linear regions and the known sample dimensions.

In Table 1 values of creep compliance, obtained from the creep data as outlined above, are given for various times of loading and for samples with various orientations.

These results are also presented graphically in Figure 2.

Discussion

The results in Figure 2 suggest that the shapes of the curves of $J(t,\theta)$ vs θ are the same for all times. To test this hypothesis a quantity J_R defined as,

$$J_R = J(t,\theta)\,\frac{J(120,45°)}{J(t,45°)} \qquad (1)$$

has been computed and its values are given in Table 2.

Close inspection of Table 2 shows that the values of J_R in each of the groups corresponding to a given value of θ do not vary in a systematic manner with time. The mean value of J_R for each group has therefore been computed and in Figure 3 is plotted against θ. The variation of the maximum and minimum values of $J(t,\theta)$ from the mean in each group is shown by the length of the vertical lines through the points. We may conclude from Figure 3 that to a first approximation, at least, J_R can be taken to be a function of θ but not of time. The anisotropic creep behaviour of this material may therefore, within the limits of this investigation, be represented by a curve of the form J_R vs θ together with one showing the variation of $\frac{J(120,45°)}{J(t,45°)}$ vs t. This latter curve is shown in Figure 4.

It is of interest to discuss the form of these two curves and in particular to discuss the form of $J_R(\theta)$. A starting point for this discussion may be found in the linear theory of elasticity for anisotropic materials (see for instance Hearmon (1961)).

Following the notation used by Hearmon (1961) (see p.3 et.seq) we may describe the stress tensor σ_{ij} in terms of six components $\sigma_1, \sigma_2, \ldots \sigma_6$ where $\sigma_1 = \sigma_{11}, \sigma_2 = \sigma_{22}, \sigma_3 = \sigma_{33}, \sigma_4 = \sigma_{23}, \sigma_5 = \sigma_{13}$ and $\sigma_6 = \sigma_{12}$, we may also describe the strain tensor ϵ_{ij} in terms of components $\epsilon_1, \epsilon_2, \ldots \epsilon_6$.

The stress-strain relation for the linear elastic case may now be written

$$\epsilon_i = S_{ij}\sigma_j \qquad (2)$$

using the usual summation convention and allowing i and j to take values from one to six. The S_{ij} are now elastic compliances.

For the case of orthorhombic symmetry equation (2) becomes

$$\begin{pmatrix} \epsilon_1 \\ \epsilon_2 \\ \epsilon_3 \\ \epsilon_4 \\ \epsilon_5 \\ \epsilon_6 \end{pmatrix} = \begin{pmatrix} S_{11} & S_{12} & S_{13} & 0 & 0 & 0 \\ & S_{22} & S_{23} & 0 & 0 & 0 \\ & & S_{33} & 0 & 0 & 0 \\ & & & S_{44} & 0 & 0 \\ & & & & S_{55} & 0 \\ & & & & & S_{66} \end{pmatrix} \begin{pmatrix} \sigma_1 \\ \sigma_2 \\ \sigma_3 \\ \sigma_4 \\ \sigma_5 \\ \sigma_6 \end{pmatrix} \quad (3)$$

For a sheet sample cut with the normal to the sheet corresponding to the three directions the elastic compliance $S(\theta)$ for tensile loading of a strip cut with its long dimensions making an angle θ to the 1 direction is

$$S(\theta) = S_{11}\cos^4\theta + (2S_{12} + S_{66})\sin^2\theta\cos^2\theta + S_{22}\sin^4\theta \quad (4)$$

These relations apply to the case of elastic deformations. In dynamic elastic deformation (i.e. without damping) S_{ij} becomes $S_{ij}(\omega)$ where ω is the (circular) frequency of the deformation.

In the linear viscoelastic theory for isotropic materials the dynamic properties of the material are represented by a complex dynamic compliance $J^*(\omega)$, see for example Ferry (1961), the real part of which $J'(\omega)$ is essentially related to the energy storage properties of the material in dynamic deformation and the imaginary part $J''(\omega)$ is related to the damping or energy loss. We will assume that in the anisotropic viscoelastic case a complex compliance can be defined which is a function of direction within the material and that this function depends upon the symmetry of the material in the same way as does the elastic compliance in the simple elastic case. We can see no support for such an assumption other than its convenience and tractability.

The complex viscoelastic compliance for an anisotropic material we will write as $J^*_{ij}(\omega)$ and for a material with orthorhombic symmetry we will expect that

$$J^*(\theta) = J^*_{11}\cos^4\theta + (2J^*_{12} + J^*_{66})\cos^2\theta\,\sin^2\theta + J^*_{22}\sin^4\theta \quad (5)$$

by analogy with equation (4) J^*_{11}, J^*_{22}, ... etc. will be complex function of ω and not functions of θ.

Now according to Gross (1953) p. 13 et seq., we may write, in the isotropic case, (and with some changes in notation).

$$J(t) = J_o + \frac{t}{\eta} + \psi(t) \quad (6)$$

in which J_o is the instantaneous compliance $J(o)$, η is a Newtonian viscosity coefficient and $\psi(t)$ a creep function such that $\psi(o) = 0$ and $\frac{d\psi}{dt} = o$ at $t = \infty$.

Similarly the dynamic compliance may be written:

$$J^*(\omega) = [J_o + J'(\omega)] + i[-\frac{1}{\omega\eta} + J''(\omega)] \tag{7}$$

From Gross (1953) p. 36 we now find the Fourier transforms:

$$\frac{d\psi(t)}{dt} = \frac{2}{\pi}\int_0^\infty J'(\omega)\cos\omega t\, d\omega = -\frac{2}{\pi}\int_0^\infty J''(\omega)\sin\omega t\, d\omega \tag{8}$$

The creep function may therefore be derived from either $J'(\omega)$, the real part of the complex dynamic modulus, or $J''(\omega)$, the imaginary part.

For the anisotropic case we proceed by writing $J_a^* = (2J_{12}^* + J_{66}^*)$ whence, adopting equations analogous to equation (7), we may write

$$J_{11}^*\cos^4\theta + J_a^*\cos^2\theta\sin^2\theta + J_{22}^*\sin^4\theta = [J_o(\theta) + J'(\omega,\theta)] + [-\frac{1}{\omega\eta(\theta)} + J''(\omega,\theta)] \tag{9}$$

or writing always $J^* = J' + i\,J''$

$$J_{11}'\cos^4\theta + J_a'\cos^2\theta\sin^2\theta + J_{22}'\sin^4\theta = J_o(\theta) + J'(\omega,\theta)$$

$$J_{11}''\cos^4\theta + J_a''\cos^2\theta\sin^2\theta + J_{22}''\sin^4\theta = -\frac{1}{\omega\eta(\theta)} + J''(\omega,\theta) \tag{10}$$

where J_{11}', J_{22}', J_a', J_{11}'', J_{22}'' and J_a'' are all functions of ω but not of θ.

Now we wish to apply Fourier transforms analogous to equations (8) to the anisotropic case. For such a procedure to be possible $J'(\infty,\theta) = o$ therefore $J_o(\theta)$ must be of the form $\alpha\cos^4\theta + \beta\sin^2\theta\cos^2\theta + \gamma\sin^4\theta$ in which α, β and γ are independent of ω and θ. It follows therefore that $J'(\omega,\theta)$ must also be of this form except that now α, β and γ are functions of ω. By a similar argument $J''(\omega,\theta)$ must be of the same form.

We now use a Fourier transform, analogous to (8), of the form

$$\frac{d\psi(t,\theta)}{dt} = \frac{2}{\pi}\int_0^\infty J'(\omega,\theta)\cos\omega t\, d\omega \tag{11}$$

writing

$$J'(\omega,\theta) = \alpha\cos^4\theta + \beta\sin^2\theta\cos^2\theta + \gamma\sin^4\theta$$

we find

$$\frac{d\psi}{dt}(t,\theta) = \cos^4\theta\int_0^\infty \alpha(\omega)\cos\omega t\, d\omega + \cos^2\theta\sin^2\theta\int_0^\infty \beta(\omega)\cos\omega t\, d\omega$$
$$+ \sin^4\theta\int_0^\infty \gamma(\omega)\cos\omega t\, d\omega \tag{12}$$

which may be written as

$$\psi(t,\theta) = \alpha(t)\cos^4\theta + \beta(t)\sin^2\theta\cos^2\theta + \Gamma(t)\sin^4\theta + K \qquad (13)$$

Noting that

$$K = K\cos^4\theta + 2K\cos^2\theta\sin^2\theta + K\sin^4\theta$$

we see that $\psi(t,\theta)$ is of the form

$$\alpha\cos^4\theta + \beta\cos^2\theta\sin^2\theta + \gamma\sin^4\theta .$$

Having established the form of $J_o(\theta)$, $\frac{1}{\eta(\theta)}$ and $\psi(t,\theta)$, it follows that $J(t,\theta)$ has the form

$$J(t,\theta) = J_{11}(t)\cos^4\theta + J_a(t)\cos^2\theta\sin^2\theta + J_{22}(t)\sin^4\theta \qquad (14)$$

In Figure 3 the curve marked 'theoretical' is computed from equation (14) with $J_{11}(t)$, $J_a(t)$ and $J_2(t)$, computed from the values of J_R at 0°, 45° and 90°.

It will be seen that the experimentally observed curve is slightly less symmetric about $\theta = 45°$ than the theoretical curve, but the deviations are not marked, and correspond to an error in θ of no more than 5°. Such an error may, at least in part, arise from poor alignment of warp and weft in the several fabric layers.

It is usual in isotropic linear viscoelastic theory to relate the creep compliance to a distribution of relaxation times $f(\tau)$ by the relation

$$\psi(t) = \int_0^\infty f(\tau)(1 - e^{-t/\tau})d\tau .$$

Let us, in the anisotropic case, choose to write

$$\psi(t,\theta) = \int_0^\infty f(\tau,\theta)(1 - e^{-t/\tau})d\tau$$

Let us further suppose that

$$f(\tau,\theta) = f_1(\tau) \times f_2(\theta)$$

then

$$\psi(t,\theta) = f_2(\theta)\int_0^\infty f_1(\tau)(1 - e^{-t/\tau})d\tau$$

$$= f_2(\theta)F(t), \quad \text{say.}$$

Now we have previously established that the creep functions $\psi(t,\theta)$ has the form given in equation (13).

It follows that we can now write

$$f_2(\theta) = \alpha \cos^4\theta + \beta \sin^2\theta\cos^2\theta + \gamma \sin^4\theta$$

in which α, β and γ are independent of both t and θ.

We have further established the form of $J_o(\theta)$ and $\frac{1}{\eta(\theta)}$. Suppose we can write

$$J_o(\theta) = J_o f_2(\theta) \quad \text{and} \quad \frac{1}{\eta(\theta)} = \frac{1}{\eta'} f_2(\theta)$$

whence

$$J(t,\theta) = f_2(\theta)[J_o' + \frac{t}{\eta'} + F(t).$$

It follows that

$$\frac{J(t,\theta)}{J(T,\theta)} = \frac{J_o' + \frac{t}{\eta'} + F(t)}{J_o' + \frac{T}{\eta'} + F(T)}$$

which is independent of θ.

The reduction of the $J(t,\theta)$ relations to the $J_R(\theta)$ relation by equation (1) is therefore consistent with a distribution of relaxation time $f(\tau,\theta)$ given by

$$f(\tau,\theta) = (\alpha \cos^4\theta + \beta\sin^2\theta\cos^2\theta + \gamma \sin^4\theta)f_1(\tau)$$

on this basis the variation of the viscoelastic properties in direction are completely prescribed.

References

1. Biot (1954) J. Appl. Phys., 25, 1385.

2. Ferry (1961) 'Viscoelastic Properties of Polymers' published Wiley - New York.

3. Gross (1953) 'Mathematical Structure of the theories of viscoelasticity' published Herman and Cie. Paris.

4. Hearmon (1961) 'Applied Anisotropic Elasticity' Published Oxford, Clarendon Press.

Table 1

Creep compliance $J(t,\theta)$ as a function of time of loading, and angle of orientation of sample with respect to the warp direction,

θ degrees / t secs	0	15	30	45	60	75	90
	Creep compliance in units of 10^{-10} $cm^2/dyne$.						
20	0.381	2.14	4.28	6.47	5.94	2.19	0.50
40	0.45	2.69	5.80	8.85	7.96	2.94	0.63
60	0.050	3.16	6.91	10.45	9.46	3.53	0.73
80	0.53	3.53	8.06	11.99	10.59	4.11	0.79
100	0.57	3.86	8.95	13.37	12.00	4.60	0.85
120	0.63	4.13	9.54	14.10	13.02	5.05	0.90

Table 2

Reduced creep compliance, $J(t,\theta)\ \frac{J(120,45°)}{J(t,45°)}$ as a function of time of loading t and angle of orientation θ.

t sec. \ θ degrees	0	15	30	45	60	75	90
	Reduced creep compliance in units 10^{-10} cm/dyne						
20	0.83	4.65	9.31	14.10	12.91	4.77	1.09
40	0.72	4.29	9.25	14.10	12.55	4.69	0.99
60	0.67	4.27	9.33	14.10	12.76	4.77	0.98
80	0.62	4.16	9.51	14.10	12.49	4.85	0.93
100	0.60	4.07	9.54	14.10	12.65	4.85	0.90
120	0.63	4.13	9.54	14.10	13.02	5.05	0.90
Mean Value	0.68	4.26	9.41	14.10	12.75	4.83	0.97
Highest Value	0.83	4.65	9.54	-	13.02	5.05	1.09
Lowest Value	0.60	4.07	9.25	-	12.49	4.69	0.90

Table 3

Reduction factor $\frac{J(120,45°)}{J(t,45°)}$ as a function of time

$\frac{J(120,45°)}{J(t,45°)}$	2.18	1.59(5)	1.35	1.18	1.05(5)	1.00
t secs	20	40	60	80	100	120

List of Captions

Figure 1 — The relation between effective creep load and creep strain at various times after application of the load for a strip cut with its long dimension at 30° to the warp direction.

Figure 2 — Creep compliance vs sample orientation for various times after application of the creep load.

Figure 3 — The reduced creep compliance, $J_R(\theta)$, vs. sample orientation. The points are the mean values of $J_R(\theta)$, at each value of orientation. The vertical lines with each point indicate the spread, maximum to minimum, in values within the group.

Figure 4 — The reduction factor as a function of time.

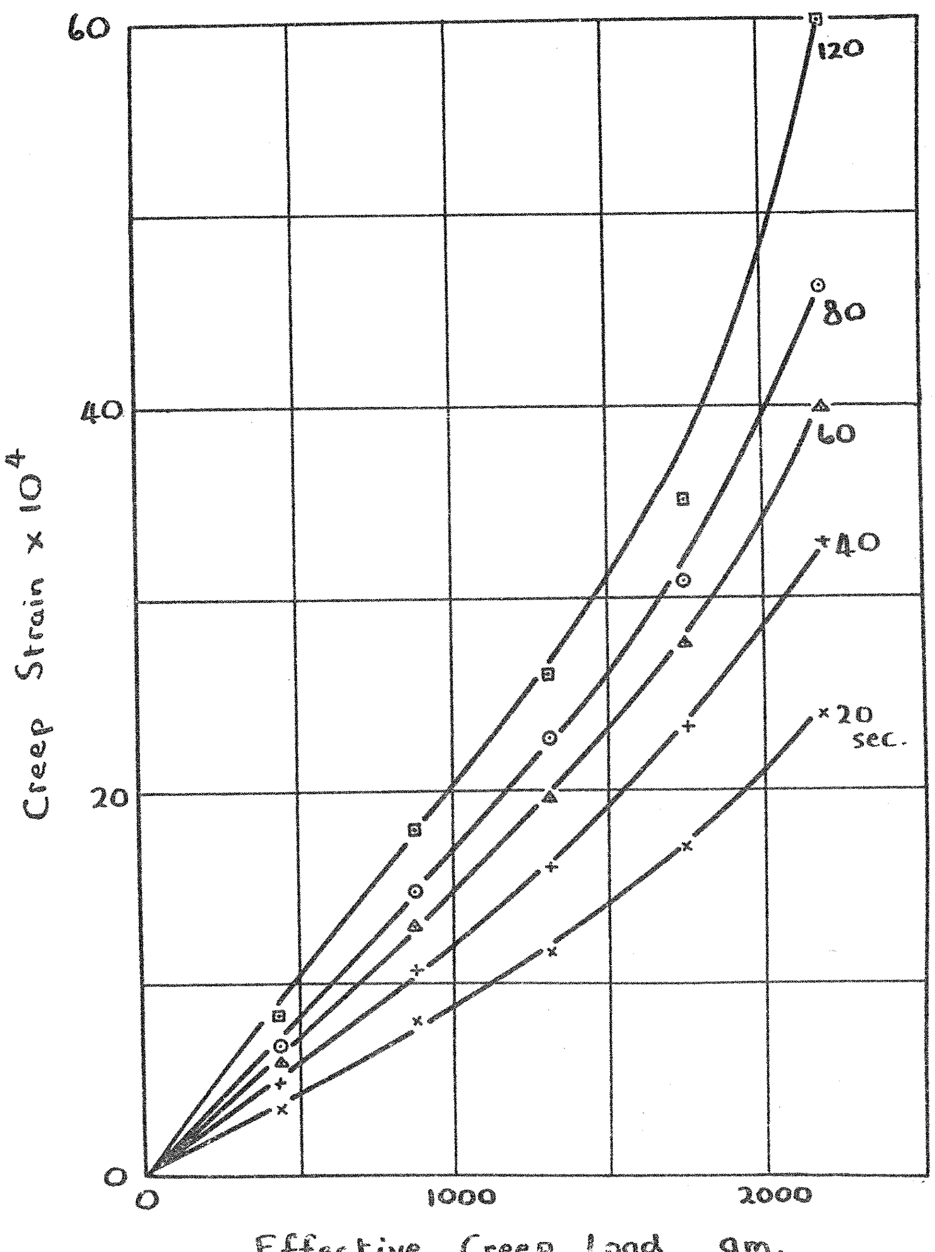

Creep Strain × 10^4
Effective Creep Load gm.
0
20
40
60
1000
2000
120
80
60
40
20 sec.

FIG. I

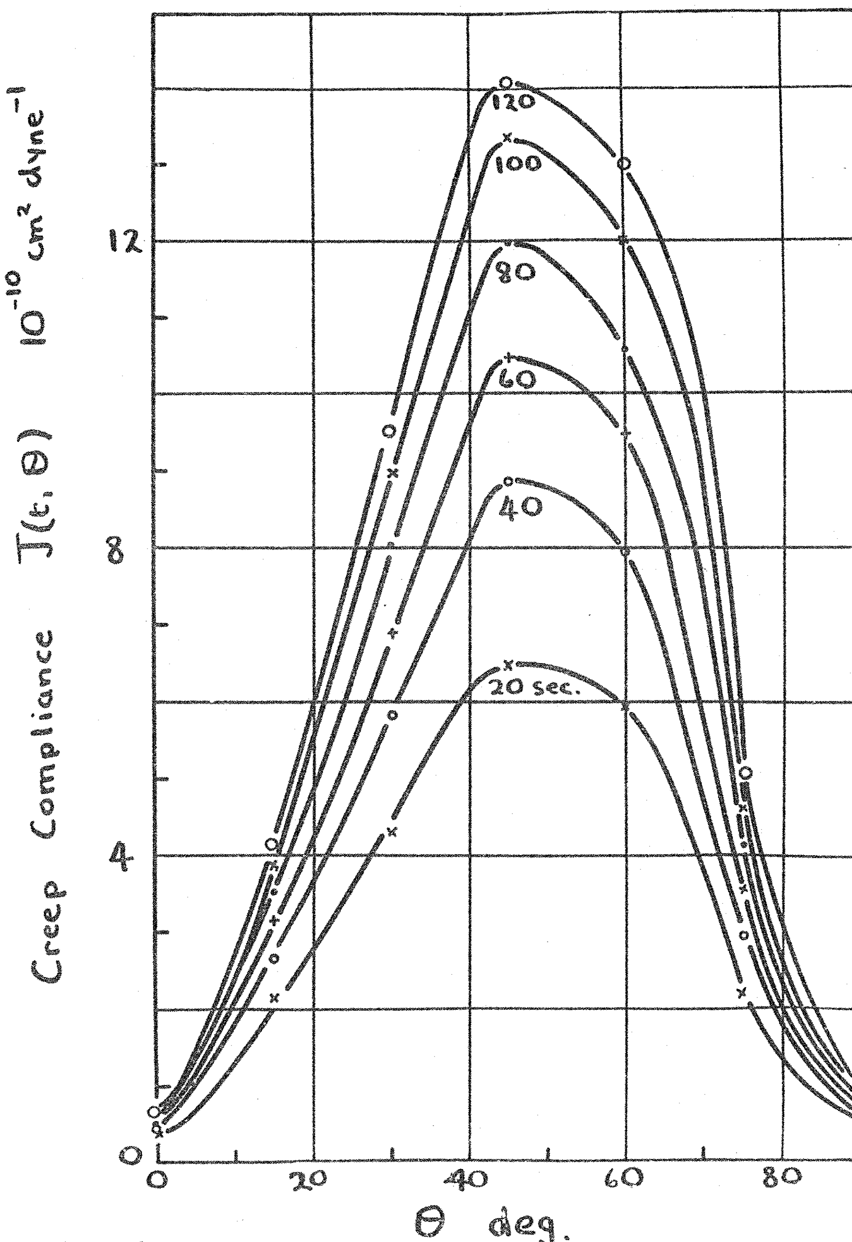

Creep Compliance $J(t, \theta)$ 10^{-10} cm^2 $dyne^{-1}$
θ deg.
0
4
8
12
20
40
60
80
120
100
80
60
40
20 sec.

FIG. 2

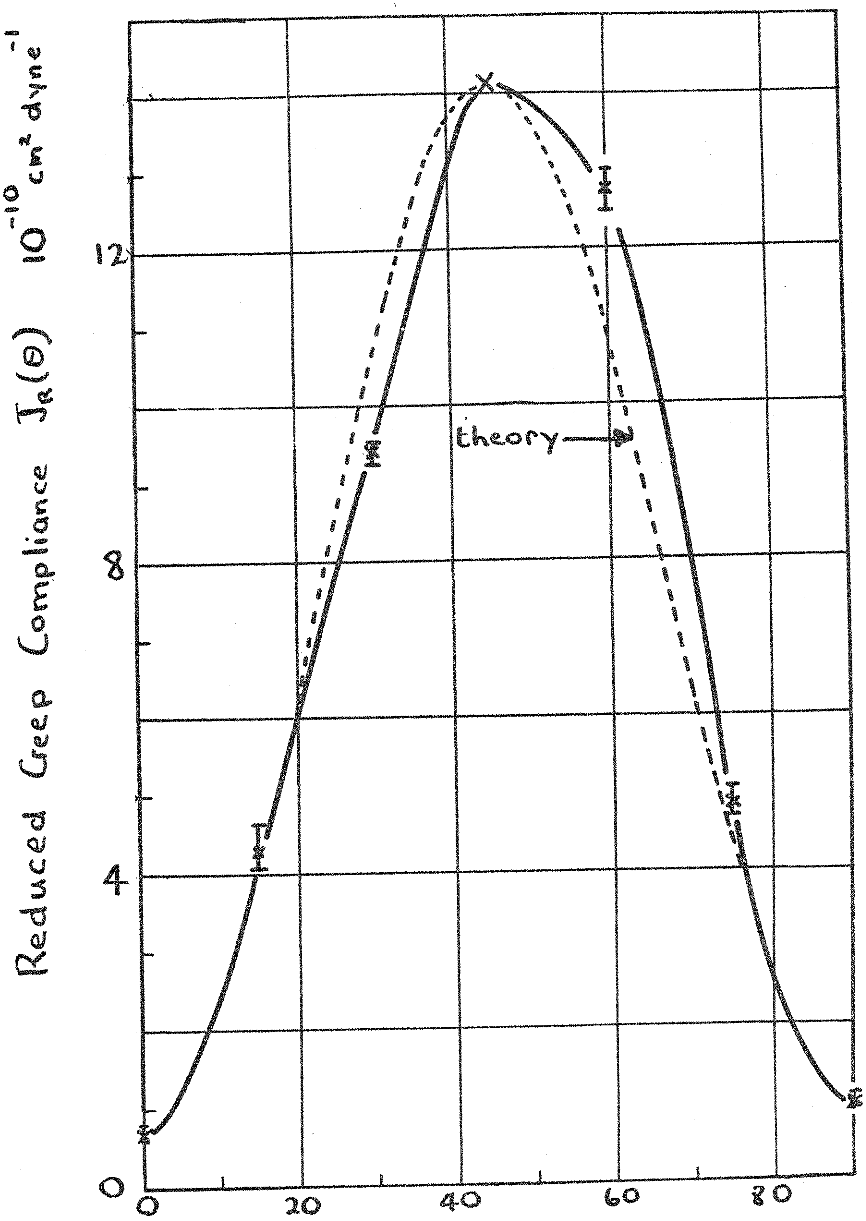

Reduced Creep Compliance $J_R(\theta)$ 10^{-10} cm^2 $dyne^{-1}$
12
8
4
0
0
20
40
60
80
θ deg.
theory

FIG. 3

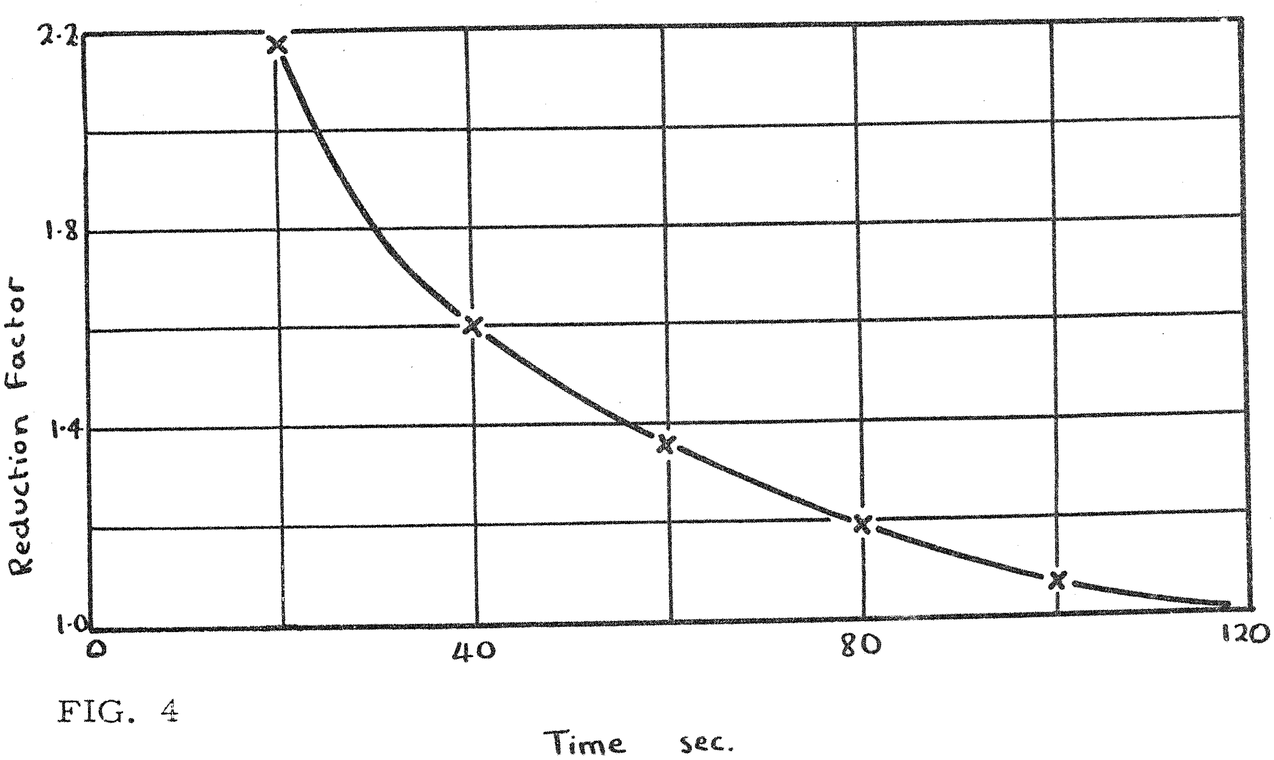

Reduction Factor
2·2
1·8
1·4
1·0
0
40
80
120
Time sec.

FIG. 4